AB Journals

African Journal of Mathematics and Statistics Studies
ISSN 2689-5323 • Volume 9, Issue 3, 2026 • pp. 129–156

REVIEW ARTICLE Received: 23 Aug 2026, Accepted: 5 Oct 2026, Published: 2 Nov 2026

Epidemiological Characteristics and Transmissibility of Brucellosis

Onyinyechi F. Anorue[1*]; Mark I. Modebei[2]; Emeka F. Obiajulu[3]

[1]Department of Mathematics, Michael Okpara University of Agriculture, Umudike, Abia State.
[2]Mathematics Programme, National Mathematical Centre, Abuja, Nigeria.
[3]Department of Mathematics, Nnamdi Azikiwe University, Awka, Anambra State.

[*]*Corresponding Author's Email: onyinyechianorue@gmail.com*

Abstract

This study investigates brucellosis transmission among humans and ruminants, together with environmental contamination, using the original nine-compartment deterministic model. The analysis examines solution properties, the disease-free and endemic equilibria, the basic reproduction number and the direction of the threshold bifurcation. For the system as formulated, the next-generation method gives a reproduction threshold that is consistent with the endemic-equilibrium existence condition: a unique positive equilibrium exists when R_0 exceeds one. A centre-manifold calculation verifies the coefficients at the critical threshold and gives a forward bifurcation. The numerical illustrations study depict the ruminant and human compartments and environmental bacterial dynamics, emphasising the relevance of ruminants and environmental exposure in brucellosis transmission. The model and results inform consideration of transmission reduction, treatment and environmental contamination control over time.

Keywords: Brucellosis, Existence and Uniqueness, Reproduction Number, Stability Analysis

How to Cite: Anorue, O. F., Modebei, M. I., & Obiajulu, E. F. (2026). Epidemiological Characteristics and Transmissibility of Brucellosis. African Journal of Mathematics and Statistics Studies, 9(3), 129–156. https://doi.org/10.52589/AJMSS-QWRGEV

© 2026 by the authors. Published by AB Journals. This is an open access article distributed under the terms of the Creative Commons Attribution (CC BY 4.0) license.

INTRODUCTION

Brucellosis is a zoonotic sexually transmitted disease that reduces the potential productivity in livestock and causes undulant fever in humans in many countries all over the world. It is considered by international organizations like the Food and Agriculture Organization (FAO), the World Health Organization (WHO), and the World Organization for Animal Health as one of the most widespread zoonoses in the world (Nyerere et al., 2020; Mpeshe et al., 2020; Esposito et al., 2023). The disease spans from the ancient, described more than 2000 years ago by the Romans, where it was first isolated in 1887 from an infected individual's blood; a British military medical officer David Bruce and thus was named Brucellosis to honour his contribution, although the disease is also known by various names like Mediterranean fever, malta fever, gastric remittent fever, Crimean fever and undulant fever due to its aftermath in human body. Brucella is classified into species, but the ones with a high rate of transmission include: B. melitensis in goats and sheep, B. abortus typically found in cattle, B. canis found in dogs, and B. suis in swine (Qureshi et al., 2024). These can also infect humans; B. melitensis remains the highest pathogenicity. Brucellosis leads to a decline in the livestock industries by causing serial abortions, sterility, decreased milk production, veterinary fees, and cost of replacing animals, retained placenta, metritis, and hygromas in chronic cases in cattle. Symptoms shared by humans include: headache, weakness, continuous or intermittent fever, chills, profuse sweats, weight loss, aches, and devastating complications that may lead to miscarriage during the first trimester of pregnancy; bone abscesses or testicular and neurological complications can occur (Nyerere et al., 2022; Zhang et al., 2019; Sun et al., 2020; Dean et al.,2012). According to the length of severity of symptoms, the disease in humans is arbitrarily classified as acute (less than 8 weeks), sub-acute (8 to 52 weeks), chronic or long-term (more than a year). Chronic signs and symptoms may include: inflammation of the inner lining of the heart chambers (endocarditis), joint inflammation (arthritis), arthritis of the spinal bones (spondylitis), arthritis of joints where the spine and pelvis connect (sacroilitis). Since the disease is commonly underestimated and debilitating in humans, the clinical signs of the disease in humans are not pathognomic; hence, patients were clinically misdiagnosed with malaria, rheumatic fever, typhoid fever, elapsing fever, and joint diseases (Galinka et al., 2013). The excretion of Brucella bacteria is in large numbers in the animal's urine, milk, placental fluid and other fluids; thus transmission of Brucella in animals is when a susceptible animal ingest contaminated materials such as pastures or discharges from infected animals while in humans, transmission is via three routes. The first transmission path is by direct contact with the skin, by handling droppings, release from the vagina, delivery through vagina and raw blood of sick animals, and by environmental contaminants (Franc, 2018). Secondly, transmission can be via the digestive tract, such as eating food, water, unpasteurized milk, and other dairy products that are contaminated by sick animals. Thirdly is through the respiratory tract. When the bacteria enter the body, mainly in the liver, spleen, bone marrow, lymphatic tissues, and other cells, they will grow, multiply, and produce endotoxin, which can cause damaged tissues. In the meantime, it often causes bacteremia and allergic reactions, but brucella does not take effect immediately when it enters the body (CDC, 2018). The immune system of humans tends to fight the bacteria when they are in small amounts, but when they exceed the threshold called a min-imum infection dose, they become harmful to the body (Pappas et al., 2006; Zhang et al., 2019; Ainseba et al., 2010; Singh, 2003). Brucella is a robust pathogen, and it can persist outside and inside mammalian hosts for a long time despite adverse conditions; it can remain in food for up to 15 months under acidic conditions and at temperatures between 14°C and 11°C, or for two to three days at 37°C. When Brucella is exposed directly to sunlight, it may survive for a few hours, while its survival in contaminated manure and aborted foetus is more than 2 months

during the winter season, (Rajendhran, 2021). Furthermore, in an ideal environment, the survival of Brucella spp. is reported to last up to 135 days (Lucero et al., 2010; Aune et al., 2012). The survival time of Brucella ranges from 1 to 4 months in contaminated soil and water, and from 2 months in milk and meat. But it can be killed by direct sunlight, high temperatures, effective disinfectants, and antibiotic treatment, which can take several weeks to months to achieve recovery. However, the infection can recur, indicating no permanent cure for someone constantly exposed to the causative agents (Li et al., 2014). In 2001, the Brazilian Ministry of Agriculture, Livestock and Food Supply (MAPA) introduced the National Program for Control and Eradication of Brucellosis and Tuberculosis (PNCEBT) to reduce the impact of Brucellosis and tuberculosis on human and animal health, and to improve the competitiveness of the Brazilian cattle industry (Lage et al., 2006).

Model Assumptions: When formulating a mathematical model, there are principles (assumptions) that are considered; these include:

i. Mixing of individuals in each population is homogeneous.

ii. Infected animals release Brucella in the environment.

iii. Domestic and wild animals' seropositivity is not lifelong and as such treatment wanes.

iv. Recovered/treated individuals may return to the susceptible compartment at the modelled waning rates.

v. The natural mortality rate in each of the species is constant.

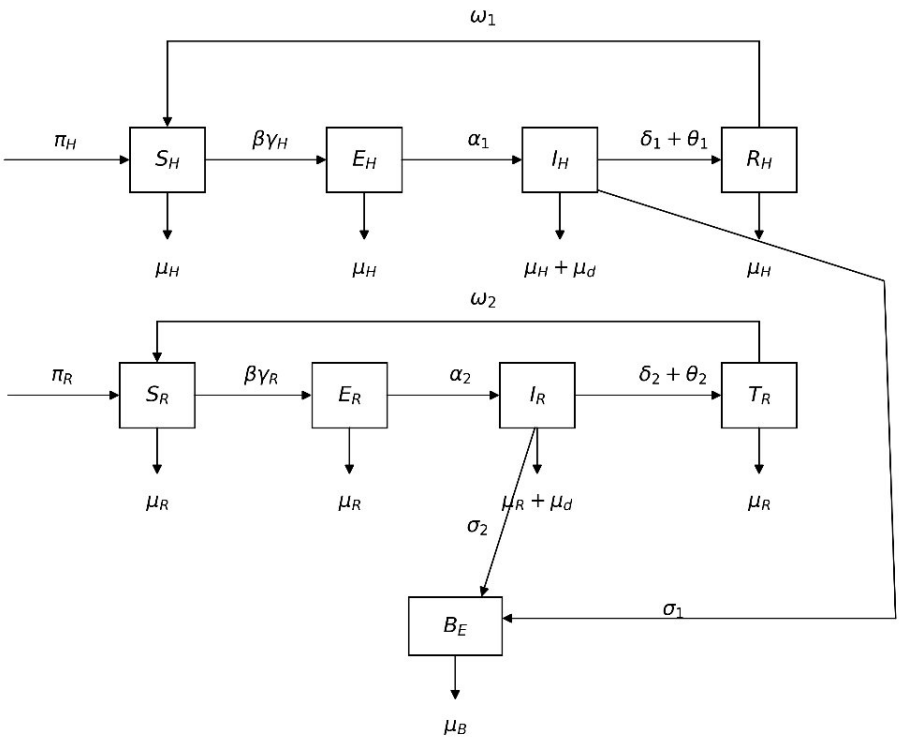


Figure 1: Compartmental flow diagram originated for the model, showing the rate of infectiousness of the subclasses

Model Formulation

Following the classical assumptions stated above, we formulate a deterministic compartmental mathematical model to describe the transmission dynamics of brucellosis, which will be an extension of the work done by Nyerere (2020). To describe the model equations, the total population $N_H(t)$ is divided into two sub-populations comprising four compartments each and a compartment for the contamination in the environment as a causative agent denoted by $B_E(t)$. The first sub-population is for the humans, which is made up of four classes: the susceptible class $S_H(t)$, the exposed class $E_H(t)$, the humans infected with the disease $I_H(t)$, and those who, through treatment, have recovered $R_H(t)$. The second sub population is for the ruminant family, which is made up of the susceptible class $S_R(t)$, the exposed class $E_R(t)$, the infected class $I_R(t)$, and the ruminants whose infections have been treated $T_R(t)$.

Model Equations

$$\frac{dS_H}{dt} = \pi_H + \omega_1 R_H - \left(\gamma_1 I_R + \gamma_2 I_H + \gamma_3 B_E\right) S_H - \mu_H S_H \tag{1}$$

$$\frac{dE_H}{dt} = \left(\gamma_1 I_R + \gamma_2 I_H + \gamma_3 B_E\right) S_H - \left(\alpha_1 + \mu_H\right) E_H \tag{2}$$

$$\frac{dI_H}{dt} = \alpha_1 E_H - \left(\delta_1 + \theta_1 + \sigma_1 + \mu_H + \mu_d\right) I_H \tag{3}$$

$$\frac{dR_H}{dt} = \left(\delta_1 + \theta_1\right) I_H - \left(\mu_H + \omega_1\right) R_H \tag{4}$$

$$\frac{dS_R}{dt} = \pi_R + \omega_2 T_R - \left(\gamma_1 I_R + \gamma_2 I_H + \gamma_3 B_E\right) S_R - \mu_R S_R \tag{5}$$

$$\frac{dE_R}{dt} = \left(\gamma_1 I_R + \gamma_2 I_H + \gamma_3 B_E\right) S_R - \left(\alpha_2 + \mu_R\right) E_R \tag{6}$$

$$\frac{dI_R}{dt} = \alpha_2 E_R - \left(\delta_2 + \theta_2 + \sigma_2 + \mu_R + \mu_d\right) I_R \tag{7}$$

$$\frac{dT_R}{dt} = \left(\delta_2 + \theta_2\right) I_R - \left(\omega_2 + \mu_R\right) T_R \tag{8}$$

$$\frac{dB_E}{dt} = \sigma_1 I_H + \sigma_2 I_R - \mu_B B_E \tag{9}$$

Where $\lambda = \left(\gamma_1 I_R + \gamma_2 I_H + \gamma_3 B_E\right)$.

Positivity of Solutions

Since the model monitors human and ruminant populations plus environmental contaminants, which are non-negative model states, all parameters and state variables used are non-negative. We now show that the model's state variables remain non-negative for all non-negative initial conditions. A feasible region Ω of a system is the set of all points in the plane that satisfy the system of inequalities, .

Consider the biological feasible region:

$$\Omega = \left\{\Omega_1 + \Omega_2 + \Omega_3 = \left(S_H, E_H, I_H, R_H, S_R, E_R, I_R, T_R, B_E \epsilon \Re_+^9 : N_H \to \frac{\pi_H}{\mu_H} \text{ and } N_R \to \frac{\pi_R}{\mu_R}\right)\right\} \quad 10.$$

Lemma1. The closed Ω is positively invariant and attracting (Anorue and Mordibei, 2020).

Proof.

Let

$(S_H(t) > 0, E_H(t) > 0, I_H(t) > 0,\ R_H(t) > 0,\ S_R(t) > 0, E_R(t) > 0, I_R(t) > 0, T_R(t) > 0,\ B_E(t) \geq 0\ )$

be the solution of the system (1)— (9), with the initial condition $(S_{0H}, E_{0H}, I_{0H}, R_{0H}, S_{0R}, E_{0R}, I_{0R}, T_{0R}, B_{0E}\ )$ and the compact set

$$\Omega = (S_H, E_H, I_H, R_H, S_R, E_R, I_R, T_R, B_E\ ) \epsilon \Re_0^9,\ L_1 \leq L_2 \leq L_3 \leq 0.$$

The region Ω is positively invariant for the model and solutions starting in Ω, approach or stay in Ω.

Using the Lyapunov function

L(t)=$\left(L_1(t), L_2(t), L_3(t)\right) = (S_H + E_H + I_H + R_H + S_R + E_R + T_R + B_E\ )$, its time derivative satisfies

$$\dot{L}(t) = \left(\dot{L_1}(t), \dot{L_2}(t), \dot{L_3}(t)\right) = \left(\dot{S_H} + \dot{E_H} + \dot{I_H} + \dot{R_H} + \dot{S_R} + \dot{E_R} + \dot{I_R} + \dot{T_R} + \dot{B_E}\right)$$

$$= \pi_H - \mu_H S_H - \mu_H E_H - \mu_H I_H - \mu_d I_H - \mu_H R_H, \pi_R - \mu_R S_R - \mu_R E_R - \mu_R I_R - \mu_d I_R - \mu_R T_R, \mu B_E.$$

$$= \pi_H - \mu_H (S_H + E_H + I_H + S_H) - \mu_d I_H, \pi_R - \mu_R (S_R + E_R + I_R + S_R) - \mu_d I_R, \ \mu B_E$$

$$\dot{L_1}(t) = \pi_H - \mu_H \dot{L_1}(t) - \mu_d I_H \leq 0 \ for L_1(t) \geq \frac{\pi_H}{\mu_H},$$

$$\dot{L_2}(t) = \pi_R - \mu_R \dot{L_2}(t) - \mu_d I_R \leq 0 \ for L_2(t) \geq \frac{\pi_R}{\mu_R} \text{ and } L_3(t) = 0$$

Hence by the above equation, we have that $\dot{L}(t) \leq 0$ which implies that Ω is a positively invariant set. On the other hand, by solving the system, we get

$$0 \leq (L_1(t), L_2(t)) \leq \left(\frac{\pi_H}{\mu_H} + L_1(0)\, e^{-\mu_H(t)}, \frac{\pi_R}{\mu_R} + L_2(0)\, e^{-\mu_H(t)}\right).$$

Where $L_1(0)$ *and* $L_2(0)$ are respectively, the initial conditions of $L_1(t)$ *and* $L_2(t)$. Thus as $t \to \infty, 0 \leq \left(L_1(t), L_2(t) \leq \left(\frac{\pi_H}{\mu_H}, \frac{\pi_R}{\mu_R}\right)\right)$ and one can conclude that Ω is an attractive set.

Existence and Uniqueness of Solution for the Model

For the mathematical model to predict the future of the system from its current state at time t_o, the initial value problem (IVP), Anorue et al., 2020.

$x' = f(t,x),\ x(t_0) = x_0$ 11

Must have a solution that exist and also unique.

So that

$x' = f(t,x) = f(x)$ 12

Theorem 1

Let D' denotes the region $|t - t_0| \leq a,\ \|x - x_0\| \leq b, x = (x_1,x_2,x_3,\ldots,x_n)$ and $x_0 = (x_{10},x_{20},\ldots..,x_{n0})$ and suppose that $f(t,x)$ satisfies the Lipschitz condition

$\|f(t.\ x_1) - f(t,x_2)\| \leq k\|x_1 - x_2\|$ 13

Whenever the pairs (t,x_1) *and* (t,x_2) belong to D', where k is a positive constant. Then, there exists a constant $\delta > 0$ such that there exist a unique continuous solution of the system (1) in the interval $|t - t_0| \leq \delta$. This can be possible following the next lemma.

Lemma 2

If $f(t,x)$ has continuous partial derivative $\frac{\partial f_i}{\partial x_j}$ on a bounded closed convex domain $\Re$. we look for a bounded solution of the form:

$0 < \Re < \infty$ 14

Since we are interested in the region

$1 \leq \varepsilon \leq \Re$ 15

We shall prove the following existence theorem.

Theorem 2

Let D^1 denote the region defined in (13) such that (14) and (15) hold, then there exists a solution of the model system(1)-(9) which is bounded in the regionD^1 .

Proof

For $f_1,f_2,\ldots.f_n$, it suffices to show that $\frac{\partial f_i}{\partial x_j},\ i,j = 1,2,3,\ldots,9$ are continuous. Consider the partial derivatives:

$\left|\frac{\partial f_1}{\partial S_H}\right| = |\gamma_1 I_R - \gamma_2 I_H - \gamma_3 B_E - \mu_H| < \infty, \left|\frac{\partial f_1}{\partial R_H}\right| = |\omega_1| < \infty, \left|\frac{\partial f_1}{\partial I_R}\right| = |-\gamma_1 S_H| < \infty, \left|\frac{\partial f_1}{\partial I_H}\right| = |-\gamma_2 S_H| < \infty, \left|\frac{\partial f_1}{\partial B_E}\right| = |-\gamma_3 S_H| < \infty, n = \left|\frac{\partial f_1}{\partial E_R}\right| = \left|\frac{\partial f_1}{\partial E_H}\right| = \left|\frac{\partial f_1}{\partial T_H}\right| = |0| < \infty.$

$$\left|\frac{\partial f_2}{\partial S_H}\right| = |\gamma_1 I_R + \gamma_2 I_H + \gamma_3 B_E| < \infty \left|\frac{\partial f_2}{\partial E_H}\right| = |-(\alpha_1 + \mu_H)| < \infty, \left|\frac{\partial f_2}{\partial I_R}\right| = |\gamma_1 S_H| < \infty, \left|\frac{\partial f_2}{\partial I_H}\right| = |\gamma_2 S_H| < \infty, \left|\frac{\partial f_2}{\partial B_E}\right| = |\gamma_3 S_H| < \infty, = \left|\frac{\partial f_2}{\partial R_H}\right| =$$

$$\left|\frac{\partial f_2}{\partial S_R}\right| = \left|\frac{\partial f_2}{\partial T_R}\right| = \left|\frac{\partial f_2}{\partial E_R}\right| = |0| < \infty.$$

$$\left|\frac{\partial f_3}{\partial E_H}\right| = |\alpha_1| < \infty, \left|\frac{\partial f_3}{\partial I_H}\right| = |-(\delta_1 + \sigma_1 + \mu_H + \mu_d)| < \infty, \left|\frac{\partial f_3}{\partial S_H}\right| = \left|\frac{\partial f_3}{\partial R_H}\right| = \left|\frac{\partial f_3}{\partial S_R}\right| = \left|\frac{\partial f_3}{\partial E_R}\right| = \left|\frac{\partial f_3}{\partial T_R}\right| = \left|\frac{\partial f_3}{\partial I_R}\right| = \left|\frac{\partial f_3}{\partial B_E}\right| = |0| < \infty$$

$$\left|\frac{\partial f_4}{\partial I_H}\right| = |\delta_1| < \infty, \left|\frac{\partial f_4}{\partial R_H}\right| = |-\mu_H| < \infty, \left|\frac{\partial f_4}{\partial S_H}\right| = \left|\frac{\partial f_4}{\partial E_H}\right| = \left|\frac{\partial f_4}{\partial S_R}\right| = \left|\frac{\partial f_4}{\partial E_R}\right| = \left|\frac{\partial f_4}{\partial I_R}\right| = \left|\frac{\partial f_4}{\partial T_R}\right| = \left|\frac{\partial f_4}{\partial B_E}\right| = |0| < \infty.$$

$$\left|\frac{\partial f_5}{\partial S_R}\right| = |-\gamma_1 I_R - \gamma_2 I_H - \gamma_3 B_E| < \infty \left|\frac{\partial f_5}{\partial I_R}\right| = |-\gamma_1 S_R| < \infty \left|\frac{\partial f_5}{\partial I_H}\right| = |-\gamma_2 S_R| < \infty \left|\frac{\partial f_5}{\partial E_R}\right| = |-\gamma_2 S_R| < \infty \left|\frac{\partial f_5}{\partial R_H}\right| = \left|\frac{\partial f_5}{\partial T_R}\right| = \left|\frac{\partial f_5}{\partial B_E}\right| =$$

$$\left|\frac{\partial f_5}{\partial E_H}\right| = \left|\frac{\partial f_5}{\partial S_H}\right| < \infty.$$

$$\left|\frac{\partial f_6}{\partial S_R}\right| = |\gamma_1 I_R + \gamma_2 I_H + \gamma_3 B_E| < \infty, \left|\frac{\partial f_6}{\partial I_R}\right| = |\gamma_1 S_R| < \infty, \left|\frac{\partial f_6}{\partial I_H}\right| = |\gamma_2 S_R| < \infty, \left|\frac{\partial f_6}{\partial E_R}\right| = |\gamma_2 S_R| < \infty, \left|\frac{\partial f_6}{\partial I_R}\right| = \left|\frac{\partial f_6}{\partial T_R}\right| = \left|\frac{\partial f_6}{\partial B_E}\right| = \left|\frac{\partial f_6}{\partial T_R}\right|$$

$$= \left|\frac{\partial f_6}{\partial B_E}\right| = |0| < \infty.$$

$$\left|\frac{\partial f_7}{\partial E_R}\right| = |\alpha_2| < \infty, \left|\frac{\partial f_7}{\partial I_R}\right| = |-(\delta_2 + \sigma_2 + \mu_R + \mu_d)| < \infty, \left|\frac{\partial f_7}{\partial I_H}\right| = \left|\frac{\partial f_7}{\partial E_R}\right| = \left|\frac{\partial f_7}{\partial I_R}\right| = \left|\frac{\partial f_7}{\partial T_R}\right| = \left|\frac{\partial f_7}{\partial B_E}\right| = \left|\frac{\partial f_7}{\partial T_R}\right| = \left|\frac{\partial f_7}{\partial B_E}\right| = |0| < \infty.$$

$$\left|\frac{\partial f_8}{\partial I_R}\right| = |\delta_2| < \infty, \left|\frac{\partial f_8}{\partial T_R}\right| = |-(\omega_2 + \mu_R)| < \infty, \left|\frac{\partial f_8}{\partial S_H}\right| = \left|\frac{\partial f_8}{\partial E_H}\right| = \left|\frac{\partial f_8}{\partial R_H}\right| = \left|\frac{\partial f_8}{\partial I_H}\right| = \left|\frac{\partial f_8}{\partial S_R}\right| = \left|\frac{\partial f_8}{\partial E_R}\right| = \left|\frac{\partial f_8}{\partial B_E}\right| = |0| < \infty.$$

$$\left|\frac{\partial f_9}{\partial I_H}\right| = |\sigma_1| < \infty, \left|\frac{\partial f_9}{\partial I_R}\right| = |\sigma_2| < \infty, \left|\frac{\partial f_9}{\partial B_E}\right| = |-\mu_B| < \infty, \left|\frac{\partial f_9}{\partial E_H}\right| = \left|\frac{\partial f_9}{\partial R_H}\right| = \left|\frac{\partial f_9}{\partial S_H}\right| = \left|\frac{\partial f_9}{\partial E_R}\right| = \left|\frac{\partial f_9}{\partial T_R}\right| = |0| < \infty.$$

Clearly all these partial derivatives are continuous and bounded. Hence, by theorem (2), there exists a unique solution of (1) – (9) in the regionD'.

Disease Free Equilibrium

Solving for the disease free-equilibrium, we equate all the model equations to zero and attend to the compartment that has no touch of infection, so that we get:

$$\rho_0 = \left(\frac{\pi_H}{\mu_H},0,0,0,\frac{\pi_R}{\mu_R},0,0,0,0\right) \tag{16}$$

Endemic Equilibrium Derivation

From equations (1)–(9), we seek a positive equilibrium X* in which the nine time derivatives vanish. The calculation can be reduced to a single non-negative equilibrium force of infection λ*.

$$D_1 = \delta_1 + \theta_1 + \sigma_1 + \mu_H + \mu_d, \qquad D_2 = \delta_2 + \theta_2 + \sigma_2 + \mu_R + \mu_d \tag{17}$$

$$\lambda^* = \gamma_1 I_R^* + \gamma_2 I_H^* + \gamma_3 B_E^* \tag{18}$$

The exposed and infectious equilibrium relations, obtained directly from equations (2), (3), (6) and (7), are:

$$E_H^* = \frac{\lambda^* S_H^*}{\alpha_1 + \mu_H}, \quad I_H^* = c_H \lambda^* S_H^*, \quad c_H = \frac{\alpha_1}{(\alpha_1 + \mu_H) D_1} \tag{19}$$

$$E_R^* = \frac{\lambda^* S_R^*}{\alpha_2 + \mu_R}, \quad I_R^* = c_R \lambda^* S_R^*, \quad c_R = \frac{\alpha_2}{(\alpha_2 + \mu_R) D_2} \tag{20}$$

Equations (4), (8) and (9) then give the recovered/treated and environmental components:

$$R_H^* = m_H I_H^*, \quad m_H = \frac{\delta_1 + \theta_1}{\mu_H + \omega_1}; \qquad T_R^* = m_R I_R^*, \quad m_R = \frac{\delta_2 + \theta_2}{\mu_R + \omega_2} \tag{21}$$

$$B_E^* = \frac{\sigma_1 I_H^* + \sigma_2 I_R^*}{\mu_B} \tag{22}$$

Substitute these expressions into the two susceptible equilibrium equations. For positive parameters, define $q_H = 1 - \omega_1 m_R c_H$ and $q_R = 1 - \omega_2 m_R c_R$. Both are strictly positive because each product $\omega_i m_i c_i$ is less than one under the stated positive transition and removal rates.

$$S_H^* = \frac{\pi_H}{\mu_H + q_H\lambda^*}, \qquad S_R^* = \frac{\pi_R}{\mu_R + q_R\lambda^*} \tag{23}$$

Define A = $\gamma_2 + \gamma_3\sigma_1/\mu_B$ and B = $\gamma_1 + \gamma_3\sigma_2/\mu_B$. From the definition of λ*, a nonzero infection force must satisfy the following one-dimensional equation:

$$1 = \Phi(\lambda^*) = \frac{Ac_H\pi_H}{\mu_H + q_H\lambda^*} + \frac{Bc_R\pi_R}{\mu_R + q_R\lambda^*} \tag{24}$$

Existence and biological feasibility. On $\lambda \geq 0$ the right-hand side $\Phi(\lambda)$ is continuous, non-negative and strictly decreasing whenever at least one effective transmission pathway is positive. It tends to zero as λ tends to infinity and satisfies $\Phi(0) = \frac{Ac_H\pi_H}{\mu_H} + \frac{Bc_R\pi_R}{\mu_R}$. Consequently, a unique $\lambda^* > 0$ exists precisely when $\Phi(0) > 1$. If $\Phi(0) \leq 1$, no positive endemic equilibrium is obtained from these equations.

$$\mathscr{R}_0 = \frac{Ac_H\pi_H}{\mu_H} + \frac{Bc_R\pi_R}{\mu_R}; \qquad \mathscr{R}_0 > 1 \Leftrightarrow \exists!\ \lambda^* > 0 \tag{25}$$

Once λ* is determined from equation (24), equations (19)–(23) recover all nine equilibrium components, and each component is non-negative. With positive recruitment and progression rates and positive effective transmission, the host components are positive. This establishes existence, uniqueness and feasibility for the endemic equilibrium of the stated system; it does not depend on a new model or a fitted parameter set.

$$X^* = \left(S_H^*, E_H^*, I_H^*, R_H^*, S_R^*, E_R^*, I_R^*, T_R^*, B_E^*\right) \tag{26}$$

Estimation of the Basic Reproduction Number

The basic reproduction number is obtained with the next-generation method using precisely the infected subsystem implied by equations (1)–(9). Environmental bacteria are included as an infection-related state, but bacterial production is classified as a transfer into the environmental reservoir, rather than counted as a newly infected host, (Anorue et al., 2020).

$$z = \left(E_H, I_H, E_R, I_R, B_E\right)^{\mathsf{T}} \tag{27}$$

At the disease-free equilibrium $X_0 = (\frac{\pi_H}{\mu_H}, 0, 0, 0, \frac{\pi_R}{\mu_R}, 0, 0, 0, 0)$, write $S_H^0 = \frac{\pi_H}{\mu_H}$, and $S_R^0 = \frac{\pi_R}{\mu_R}$. The Jacobian matrices F and V, ordered as in equation (27.1), are:

$$F = \begin{pmatrix} 0 & \gamma_2 S_H^0 & 0 & \gamma_1 S_H^0 & \gamma_3 S_H^0 \\ 0 & 0 & 0 & 0 & 0 \\ 0 & \gamma_2 S_R^0 & 0 & \gamma_1 S_R^0 & \gamma_3 S_R^0 \\ 0 & 0 & 0 & 0 & 0 \\ 0 & 0 & 0 & 0 & 0 \end{pmatrix} \tag{27.1}$$

$$V=\begin{pmatrix}\alpha_1+\mu_H & 0 & 0 & 0 & 0\\ -\alpha_1 & D_1 & 0 & 0 & 0\\ 0 & 0 & \alpha_2+\mu_R & 0 & 0\\ 0 & 0 & -\alpha_2 & D_2 & 0\\ 0 & -\sigma_1 & 0 & -\sigma_2 & \mu_B\end{pmatrix} \tag{27.2}$$

Here F contains the two host-incidence terms and V contains progression, removal and environmental bacterial transfer. V is invertible for strictly positive progression and removal rates. The next-generation matrix is $K = FV^{-1}$. Because F has two nonzero rows, the nonzero eigenvalues of K coincide with those of the following 2×2 effective host matrix:

$$M=\begin{pmatrix}S_H^0 Ac_H & S_H^0 Bc_R\\ S_R^0 Ac_H & S_R^0 Bc_R\end{pmatrix},\quad A=\gamma_2+\frac{\gamma_3\sigma_1}{\mu_B}, B=\gamma_1+\frac{\gamma_3\sigma_2}{\mu_B} \tag{27.3}$$

The two rows are proportional because equations (1)–(9) use the same infection pressure for susceptible humans and susceptible ruminants. Thus det(M) = 0 and its eigenvalues are 0 and tr(M); this is an algebraic consequence of the ORIGINAL incidence specification, not an imposed assumption.

$$\mathscr{R}_0=\rho(K)=\rho(M)=S_H^0 Ac_H+S_R^0 Bc_R \tag{27.4}$$

$$\mathscr{R}_0=\frac{\pi_H\alpha_1\left(\gamma_2+\gamma_3\sigma_1/\mu_B\right)}{\mu_H\left(\alpha_1+\mu_H\right)D_1}+\frac{\pi_R\alpha_2\left(\gamma_1+\gamma_3\sigma_2/\mu_B\right)}{\mu_R\left(\alpha_2+\mu_R\right)D_2} \tag{28}$$

The disease-free equilibrium is locally asymptotically stable when $R_0 < 1$ and unstable when $R_0 > 1$, by the next-generation threshold result. At $R_0 = 1$ the linearisation has a zero eigenvalue, and the threshold is examined using the centre-manifold calculation in Section 1.10. The formula in equation (28) is also the value $\Phi(0)$ appearing in the endemic-equilibrium condition (25), providing an internal consistency check.

$$\mathscr{R}_0<1\Rightarrow \text{local stability of } X_0;\qquad \mathscr{R}_0>1\Rightarrow \text{instability of } X_0 \tag{29}$$

Stability of Disease Free Equilibrium

To examine the local stability of the disease free equilibriumρ_0, we evaluate the Jacobian matrix at ρ_0 to get:

$$J(\varepsilon_0)=\begin{pmatrix}-\mu_H & 0 & -\gamma_2 S_H^0 & & & & -\gamma_1 S_H^0 & 0 & -\gamma_3 S_H^0\\ 0 & -(\alpha_1+\mu_H) & \gamma_2 S_H^0 & \omega_1 & 0 & 0 & \gamma_1 S_H^0 & 0 & \gamma_3 S_H^0\\ & & -D_1 & 0 & 0 & 0 & 0 & & 0\\ 0 & \alpha_1 & \Gamma_1 & -(\mu_H+\omega_1) & 0 & 0 & 0 & 0 & 0\\ 0 & 0 & & 0 & -\mu_R & 0 & -\gamma_1 S_R^0 & 0 & -\gamma_3 S_R^0\\ 0 & 0 & \gamma_2 S_R^0 & 0 & 0 & -(\alpha_2+\mu_H) & \gamma_1 S_R^0 & \omega_2 & \gamma_3 S_R^0\\ 0 & 0 & \gamma_2 S_R^0 & 0 & 0 & \alpha_2 & -D_2 & 0 & 0\\ 0 & 0 & 0 & 0 & 0 & 0 & \Gamma_2 & -(\omega_2+\mu_R) & 0\\ 0 & 0 & 0 & 0 & 0 & 0 & \sigma_2 & 0 & -\mu_B\\ & & \sigma_1 & & & & & & \end{pmatrix}$$

Where $S_H^0 = \frac{\pi_H}{\mu_H},\ S_R^0 = \frac{\pi_H}{\mu_R}$.

Eigenvalue Analysis at DFE

The characteristic equation is:

$$\det(J(\varepsilon_0) - \lambda I_9) = 0 \qquad (30)$$

Since the matrix has block structure, the eigenvalues can be grouped: Susceptible compartments (S_H, S_R)

From rows 1 and 5, columns 1 and 5:

$$\begin{vmatrix} -\mu_H - \lambda & 0 \\ 0 & -\mu_R - \lambda \end{vmatrix} = (\lambda + \mu_H)(\lambda + \mu_R) = 0$$

Gives eigenvalues: $\lambda_1 = -\mu_H,\ \lambda_2 = -\mu_R\ (both\ negative)$.

Recovered compartments (R_H, T_R): From rows 4 and 8, columns 4 and 8:

$$\begin{vmatrix} -(\mu_H + \omega_1) - \lambda & 0 \\ 0 & -(\omega_2 + \mu_R) - \lambda \end{vmatrix} = [\lambda + (\mu_H + \omega_1)][\lambda + (\omega_2 + \mu_R)] = 0$$

Gives eigenvalues: $\lambda_3 = -(\mu_H + \omega_1),\ \lambda_4 = -(\omega_2 + \mu_R)\ (both\ negative)$.

Infected compartments $(E_H, I_H, E_R, I_R, B_E)$

This is a 5 x 5 sub-matrix:

$$J_{inf}(\varepsilon_0) = \begin{pmatrix} -(\alpha_1 + \mu_H) & \gamma_2 S_H^0 & 0 & \gamma_1 S_H^0 & \gamma_3 S_H^0 \\ \alpha_1 & -D_1 & 0 & 0 & 0 \\ 0 & \gamma_2 S_R^0 & -(\alpha_2 + \mu_R) & \gamma_1 S_R^0 & \gamma_3 S_R^0 \\ 0 & 0 & \alpha_2 & -D_2 & 0 \\ 0 & \sigma_1 & 0 & \sigma_2 & -\mu_B \end{pmatrix}$$

The stability of DFE depends on the eigenvalues of J_{inf}. According to the Next Generation Matrix method, all eigenvalues of J_{inf} have negative real parts if and only $\mathscr{R}_0 < 1$.

Characteristic Polynomial for Infected Subsystem: The characteristic polynomial for J_{inf} is:

$$P(\lambda) = \det(J_{inf} - \lambda I_5) \qquad (31)$$

Expanding:

By Routh-Hurwitz Stability Criterion for DFE stability $\mathscr{R}_0 < 1$, we need all roots to have negative real parts. The characteristic polynomial is of degree 5:

$$P(\lambda) = \lambda^5 + \alpha_1\lambda^4 + \alpha_2\lambda^3 + \alpha_3\lambda^2 + \alpha_4\lambda + \alpha_5 \qquad (32)$$

The Routh-Hurwitz conditions for stability are:

1. $a_i > 0$ for $i = 1,2,3,4,5$
2. $a_1 a_2 - a_3 > 0$
3. $(a_1 a_2 - a_3) a_3 - a_1^2 a_4 + a_1 a_5 > 0$
4. $a_4 > 0$ and $a_5 > 0$ |
5. All principal minors of the Routh Hurwitz matrix are positive

Bifurcation Analysis

We verify the Castillo-Chavez and Song (2004) coefficients for the nonlinear system (1)–(9). Let $\beta = \gamma_2$ be the bifurcation parameter, and assume a positive critical value β^* for which $R_0(\beta^*) = 1$, with the remaining rates positive. Let $f(x,\beta)$ be the nine-dimensional right-hand side in the order $x = (S_H, E_H, I_H, R_H, S_R, E_R, I_R, T_R, B_E)$.

$$\mathscr{R}_0(\beta^*) = S_H^0 c_H \left(\beta^* + \frac{\gamma_3 \sigma_1}{\mu_B}\right) + S_R^0 c_R \left(\gamma_1 + \frac{\gamma_3 \sigma_2}{\mu_B}\right) = 1 \tag{33}$$

Set $A^* = \beta^* + \gamma_3\sigma_1/\mu_B$, $B = \gamma_1 + \gamma_3\sigma_2/\mu_B$ and retain m_H, m_R, q_H, q_R, c_H *and* c_R from Section 1.7. At $\beta = \beta^*$ a right zero-eigenvector v can be scaled so that the corresponding perturbation of the force of infection is one:

$$v_{I_H} = S_H^0 c_H, \quad v_{I_R} = S_R^0 c_R, \quad v_{B_E} = \frac{\sigma_1 v_{I_H} + \sigma_2 v_{I_R}}{\mu_B} \tag{34}$$

$$v_{E_H} = \frac{S_H^0}{\alpha_1 + \mu_H}, \quad v_{E_R} = \frac{S_R^0}{\alpha_2 + \mu_R}, \quad v_{R_H} = m_H v_{I_H}, \quad v_{T_R} = m_R v_{I_R} \tag{34.1}$$

$$v_{S_H} = -\frac{q_H S_H^0}{\mu_H}, \qquad v_{S_R} = -\frac{q_R S_R^0}{\mu_R} \tag{34.2}$$

These relations solve $J(X_0,\beta^*)v = 0$. In particular, $\gamma_2 * v_{I_H} + \gamma_1 v_{I_R} + \gamma_3 v_{B_E} = R_0(\beta *) = 1$. A left zero-eigenvector w has zero components for S_H, R_H , S_R and T_R. Its remaining components, prior to normalisation, may be taken as:

$$\tilde{w}_{E_H} = A^* c_H, \quad \tilde{w}_{I_H} = \frac{A^*}{D_1}, \quad \tilde{w}_{E_R} = B c_R, \quad \tilde{w}_{I_R} = \frac{B}{D_2}, \quad \tilde{w}_{B_E} = \frac{\gamma_3}{\mu_B} \tag{35}$$

Define $N = \tilde{w}\cdot v > 0$ and $w = \tilde{w}/N$, so that $w\cdot v = 1$. The normalisation also gives $\tilde{w}_{E_H} S_H^0 + \tilde{w}_{E_R} S_R^0 = 1$. Thus the only nonlinear terms that contribute to the centre-manifold coefficient a are the bilinear host-incidence expressions λS_H and λS_R in the exposed-compartment equations.

$$a_{CM} = \sum_{k,i,j} w_k v_i v_j \left. \frac{\partial^2 f_k}{\partial x_i \partial x_j} \right|_{(X_0, \beta^*)} \tag{36}$$

$$b_{CM} = \sum_{k,i} w_k v_i \left. \frac{\partial^2 f_k}{\partial x_i \partial \beta} \right|_{(X_0, \beta^*)} \tag{37}$$

Forb_{CM} , the only nonzero mixed derivatives weighted by w are $\frac{\partial^2 f_{E_H}}{\partial I_H \partial \beta} = S_H^0$ and $\frac{\partial^2 f_{E_R}}{\partial I_H \partial \beta} = S_R^0$.

Consequently

$$b_{CM} = \frac{v_{I_H}}{N}\left(\tilde{w}_{E_H} S_H^0 + \tilde{w}_{E_R} S_R^0\right) = \frac{S_H^0 c_H}{N} > 0 \tag{38}$$

For a_{CM}, the nonzero quadratic terms weighted by w are the second derivatives of λS_H and λS_R Since the infection-force perturbation is one, the calculation simplifies to:

$$a_{CM} = \frac{2}{N}\left(\tilde{w}_{E_H} v_{S_H} + \tilde{w}_{E_R} v_{S_R}\right) \tag{39}$$

$$a_{CM} = -\frac{2}{N}\left(\frac{A^* c_H q_H S_H^0}{\mu_H} + \frac{B c_R q_R S_R^0}{\mu_R}\right) < 0 \tag{40}$$

Because $a_{CM} < 0$ and $b_{CM} > 0$ at a positive simple threshold, the Castillo-Chavez–Song criterion yields a forward (transcritical) bifurcation. This sign result follows from the same host and environmental equations used in the original manuscript. The earlier statement of a backward bifurcation, especially under the no-cross-transmission special case, does not follow from this system and therefore cannot be retained as a verified mathematical conclusion.

$$a_{CM} < 0, \quad b_{CM} > 0 \quad \Rightarrow \quad \text{forward bifurcation at } \mathscr{R}_0 = 1 \tag{41}$$

This calculation establishes the direction of the local branch near the threshold; global asymptotic stability of a general endemic equilibrium is a separate proposition requiring its own valid Lyapunov or equivalent argument. No additional epidemiological compartments, transmission routes or replacement numerical simulations have been introduced in this verification.

Global Stability of Disease-Free Equilibrium

Theorem 3 (Global Stability of DFE). If $\mathscr{R}_0 \leq 1$,

then the Disease-Free Equilibrium $\mathscr{E}_0$ is globally asymptotically stable in the feasible region Ω.

Proof: We construct a Lyapunov function of the form:

$$L = a_1 E_H + a_2 I_H + a_3 E_R + a_4 I_R + a_5 B_E + a_6 \left(S_H - S_H^0\right)^2 + a_7 \left(S_R - S_R^0\right)^2$$

where $S_H^0 = \frac{\pi_H}{\mu_H}, S_R^0 = \frac{\pi_R}{\mu_R}$, and $a_i > 0$ are constants to be determined.

Time derivative along trajectories

$$\begin{aligned}\frac{dL}{dt} =& a_1 \frac{dE_H}{dt} + a_2 \frac{dI_H}{dt} + a_3 \frac{dE_R}{dt} + a_4 \frac{dI_R}{dt} + a_5 \frac{dB_E}{dt} \\ &+ 2a_6 \left(S_H - S_H^0\right) \frac{dS_H}{dt} + 2a_7 \left(S_R - S_R^0\right) \frac{dS_R}{dt}\end{aligned}$$

Substitute derivatives

$$\begin{aligned}\frac{dL}{dt} =& a_1 \left[\lambda_H S_H - \left(\alpha_1 + \mu_H\right) E_H\right] + a_2 \left[\alpha_1 E_H - D_1 I_H\right] \\ &+ a_3 \left[\lambda_R S_R - \left(\alpha_2 + \mu_R\right) E_R\right] + a_4 \left[\alpha_2 E_R - D_2 I_R\right] \\ &+ a_5 \left[\sigma_1 I_H + \sigma_2 I_R - \mu_B B_E\right] \\ &+ 2a_6 \left(S_H - S_H^0\right) \left[\pi_H + \omega_1 R_H - \lambda_H S_H - \mu_H S_H\right] \\ &+ 2a_7 \left(S_R - S_R^0\right) \left[\pi_R + \omega_2 T_R - \lambda_R S_R - \mu_R S_R\right]\end{aligned}$$

Using equilibrium conditions, at DFE: $\pi_H = \mu_H S_H^0, \pi_R = \mu_R S_R^0$.

Also, near DFE, $S_H \leq S_H^0, S_R \leq S_R^0$.

Rewrite the last two terms:

$$\begin{aligned}&\pi_H + \omega_1 R_H - \lambda_H S_H - \mu_H S_H \\ &= \mu_H S_H^0 + \omega_1 R_H - \lambda_H S_H - \mu_H S_H \\ &= \mu_H \left(S_H^0 - S_H\right) + \omega_1 R_H - \lambda_H S_H\end{aligned}$$

Similarly for ruminants.

Choose coefficients a_i

We want to express $\frac{dL}{dt}$ in terms of $\mathscr{R}_0 - 1$. Choose:

$$a_1 = \frac{1}{\alpha_1 + \mu_H}, a_2 = \frac{1}{D_1}, a_3 = \frac{1}{\alpha_2 + \mu_R}, a_4 = \frac{1}{D_2}, a_5 = \frac{1}{\mu_B}$$

Then:

$$\begin{aligned}\frac{dL}{dt} \leq& \lambda_H S_H \left(\frac{1}{\alpha_1 + \mu_H}\right) + \frac{\alpha_1}{\alpha_1 + \mu_H} E_H - E_H - \frac{D_1}{D_1} I_H \\ &+ \lambda_R S_R \left(\frac{1}{\alpha_2 + \mu_R}\right) + \frac{\alpha_2}{\alpha_2 + \mu_R} E_R - E_R - \frac{D_2}{D_2} I_R \\ &+ \frac{\sigma_1}{\mu_B} I_H + \frac{\sigma_2}{\mu_B} I_R - B_E \\ &+ 2a_6 \left(S_H - S_H^0\right) \left[\mu_H \left(S_H^0 - S_H\right) + \omega_1 R_H - \lambda_H S_H\right] \\ &+ 2a_7 \left(S_R - S_R^0\right) \left[\mu_R \left(S_R^0 - S_R\right) + \omega_2 T_R - \lambda_R S_R\right]\end{aligned}$$

We simplify using inequalities, since $S_H \le S_H^0$ and $S_R \le S_R^0$ in Ω, and $R_H, T_R \ge 0$-:

$$\left(S_H - S_H^0\right)\left[\mu_H\left(S_H^0 - S_H\right) + \omega_1 R_H - \lambda_H S_H\right] \le -\mu_H\left(S_H - S_H^0\right)^2 - \lambda_H S_H\left(S_H - S_H^0\right)$$
$$\left(S_R - S_R^0\right)\left[\mu_R\left(S_R^0 - S_R\right) + \omega_2 T_R - \lambda_R S_R\right] \le -\mu_R\left(S_R - S_R^0\right)^2 - \lambda_R S_R\left(S_R - S_R^0\right)$$

We combine terms

$$\begin{aligned}\frac{dL}{dt} \le & \lambda_H S_H^0\left(\frac{1}{\alpha_1 + \mu_H}\right) - I_H + \frac{\alpha_1}{\alpha_1 + \mu_H} E_H - E_H \\ & + \lambda_R S_R^0\left(\frac{1}{\alpha_2 + \mu_R}\right) - I_R + \frac{\alpha_2}{\alpha_2 + \mu_R} E_R - E_R \\ & + \frac{\sigma_1}{\mu_B} I_H + \frac{\sigma_2}{\mu_B} I_R - B_E \\ & - 2a_6\mu_H\left(S_H - S_H^0\right)^2 - 2a_7\mu_R\left(S_R - S_R^0\right)^2 \\ & - 2a_6\lambda_H S_H\left(S_H - S_H^0\right) - 2a_7\lambda_R S_R\left(S_R - S_R^0\right)\end{aligned}$$

Express in terms of $\mathscr{R}_0$

Recall that at DFE:

$$\lambda_H S_H^0 = \left(\gamma_1 I_R + \gamma_2 I_H + \gamma_3 B_E\right) S_H^0 ; \lambda_R S_R^0 = \left(\gamma_1 I_R + \gamma_2 I_H + \gamma_3 B_E\right) S_R^0$$

Choose a_6 *and* a_7 sufficiently small so that the cross terms are dominated. Then:

$$\begin{aligned}&\frac{dL}{dt} \\ &\le \left(\frac{\gamma_2 S_H^0}{\alpha_1 + \mu_H} + \frac{\gamma_2 S_R^0}{\alpha_2 + \mu_R} + \frac{\sigma_1}{\mu_B} - 1\right) I_H + \left(\frac{\gamma_1 S_H^0}{\alpha_1 + \mu_H} + \frac{\gamma_2 S_R^0}{\alpha_2 + \mu_R} + \frac{\sigma_2}{\mu_B} - 1\right) I_R \\ &+ \left(\frac{\gamma_3 S_H^0}{\alpha_1 + \mu_H} + \frac{\gamma_3 S_R^0}{\alpha_2 + \mu_R} - 1\right) B_E - \textit{ positive terms in } (S_H - S_H^0)^2, (S_R - S_R^0)^2\end{aligned}$$

Relating to $\mathscr{R}_0$from the Next Generation Matrix analysis:

$$\mathscr{R}_0 = \max\left\{\frac{\gamma_2 S_H^0 \alpha_1}{(\alpha_1 + \mu_H) D_1} + \frac{\gamma_1 S_H^0 \alpha_2}{(\alpha_2 + \mu_R) D_2} + \frac{\gamma_3 S_H^0}{\mu_B}\left(\frac{\alpha_1 \sigma_1}{(\alpha_1 + \mu_H) D_1} + \frac{\alpha_2 \sigma_2}{(\alpha_2 + \mu_R) D_2}\right), \ \ldots\right\}$$

When $\mathscr{R}_0 \le 1$, we can show that:

$$\frac{\gamma_2 S_H^0}{\alpha_1 + \mu_H} + \frac{\sigma_1}{\mu_B} < 1; \frac{\gamma_1 S_H^0}{\alpha_1 + \mu_H} + \frac{\sigma_2}{\mu_B} < 1; \frac{\gamma_3 S_H^0}{\alpha_1 + \mu_H} < 1$$

Thus $\frac{dL}{\mathrm{dt}} \le 0$ *when* $\mathscr{R}_0 \le 1$.

LaSalle's Invariance Principle

Let $E = \left\{\left(S_H, E_H, I_H, R_H, S_R, E_R, I_R, T_R, B_E\right) \in \Omega: \frac{dL}{\mathrm{dt}} = 0\right\}$.

$\frac{dL}{\mathrm{dt}} = 0$ *implies*:

- $S_H = S_H^0, S_R = S_R^0$
- $I_H = I_R = B_E = 0$
- *Then from equations*: $E_H = E_R = R_H = T_R = 0$

Thus $E = \{\varepsilon_0\}$.

By LaSalle's Invariance Principle, ε_0 *is globally asymptotically stable in* Ω *when* $\mathscr{R}_0 \leq 1$.

Global Stability of Endemic Equilibrium

Theorem 4 (Global Stability of EE): If $\mathscr{R}_0 > 1$, then the Endemic Equilibrium ε^* is globally asymptotically stable in the interior of Ω.

Proof: We construct a Volterra-type Lyapunov function defined as:

$$V = \sum_{i=1}^{9} c_i \left(1 - \frac{x_i^*}{x_i}\right) \sum_{i=1}^{9} c_i$$

$$\left(x_i - x_i^* - x_i^* \, In \, \frac{x_i}{x_i^*}\right) \tag{45}$$

where $x = \left(S_H, E_H, I_H, R_H, S_R, E_R, I_R, T_R, B_E\right)$, $x^*$are EE values, and $c_i > 0$ are constants. Compute time derivative

$$\frac{dV}{dt} = \sum_{i=1}^{9} c_i \left(1 - \frac{x_i^*}{x_i}\right) \frac{dx_i}{dt} = \sum_{i=1}^{9} c_i \frac{x_i - x_i^*}{x_i} \tag{45.1}$$

Write each term using equilibrium conditions. At EE:

$$\pi_H = \lambda_H^* S_H^* + \pi_H S_H^* - \omega_1 R_H^* \tag{45.2}$$

$$\omega_2 + \mu_R = \frac{\Gamma_2 I_R^*}{T_R^*}$$

$$\mu_B = \frac{\sigma_1 I_H^* + \sigma_2 I_R^*}{B_R^*}$$

Where $\lambda_H^* = \lambda_1 I_R^* + \lambda_2 I_H^* + \lambda_3 B_E^*$, $\lambda_R^* = \lambda_1 I_R^* + \lambda_2 I_H^* + \lambda_3 B_E^*$.

First term $\left(S_H\right)$

$$c_1 \frac{S_H - S_H^*}{S_H} \frac{dS_H}{\mathrm{dt}} = c_1 \frac{S_H - S_H^*}{S_H} \left[\pi_H + \omega_1 R_H - \lambda_H S_H = \mu_H S_H\right]$$

$$= c_1\left[\lambda_2^* S_H^*\left(\frac{S_H - S_H^*}{S_H}\right) + \pi_H S_H^*\left(\frac{S_H - S_H^*}{S_H}\right) - \omega_1 R_H^*\left(\frac{S_H - S_H^*}{S_H}\right) + \omega_1 R_H\left(\frac{S_H - S_H^*}{S_H}\right) - \lambda_H\left(S_H - S_H^*\right) - \pi_H\left(S_H - S_H^*\right)\right]$$

(45.3)

Second term (E_H)

$$c_2\frac{E_H - E_H^*}{E_H}\frac{dE_H}{\mathrm{dt}} = c_2\frac{E_H - E_H^*}{E_H}\left[\lambda_H S_H - \left(\alpha_1 + \mu_H\right)E_H\right] \Rightarrow c_2\frac{E_H - E_H^*}{E_H}\left[\lambda_H S_H - \frac{\lambda_H^* S_H^*}{E_H^*}E_H\right]$$

(45.4)

Third term (I_H)

$$c_3\frac{I_H - I_H^*}{I_H}\frac{dI_H}{\mathrm{dt}} = c_3\frac{I_H - I_H^*}{I_H}\left[\alpha_1 E_H - D_1 I_H\right] = c_3\frac{I_H - I_H^*}{I_H}\left[\alpha_1 E_H - \frac{\alpha_1 E_H^*}{I_H^*}I_H\right] \quad (45.5)$$

Fourth term (R_H)

$$c_4\frac{R_H - R_H^*}{R_H}\frac{dR_H}{\mathrm{dt}} = c_4\frac{R_H - R_H^*}{R_H}\left[\Gamma_1 I_H - \left(\mu_H + \omega_1\right)R_H\right]$$

$$\Rightarrow \quad c_4\frac{R_H - R_H^*}{R_H}\left[\Gamma_1 I_H - \frac{\Gamma_1 I_H^*}{R_H^*}R_H\right] \quad (45.6)$$

Fifty term (S_R)

Similar to S_H:

$$c_5\frac{S_R - S_R^*}{S_R}\frac{dS_R}{\mathrm{dt}} = c_5\frac{S_R - S_R^*}{S_R}\left[\left(\lambda_R^* S_R^* + \mu_R S_R^* - \omega_2 T_R^*\right) + \omega_2 T_R^* - \lambda_R S_R - \mu_R S_R\right] \quad (45.7)$$

Sixth term (E_R)

$$c_6\frac{E_R - E_R^*}{E_R}\frac{dE_R}{\mathrm{dt}} = c_6\frac{E_R - E_R^*}{E_R}\left[\lambda_R S_R - \frac{\lambda_R^* S_R^*}{E_R^*}E_R\right] \quad (45.8)$$

Seventh term (I_R)

$$c_7\frac{I_R - I_R^*}{I_R}\frac{dI_R}{\mathrm{dt}} = c_7\frac{I_R - I_R^*}{I_R}\left[\alpha_2 E_R - \frac{\alpha_2 E_R^*}{I_R^*}I_R\right] \quad (45.9)$$

Eighth term (T_R)

$$= c_8\frac{T_R - T_R^*}{T_R}\frac{dT_R}{\mathrm{dt}} = c_8\frac{T_R - T_R^*}{T_R}\left[\Gamma_2 I_R - \frac{\Gamma_2 I_R^*}{T_R^*}T_R\right] \quad (45.10)$$

Ninth term (T_R)

$$c_9\frac{B_E - B_E^*}{B_E}\frac{dB_E}{\mathrm{dt}}$$

$$= c_9 \frac{B_E - B_E^*}{B_E} \left[\sigma_1 I_H - \sigma_2 I_R - \mu_B B_E\right]$$

$$= c_9 \frac{B_E - B_E^*}{B_E} \left[\sigma_1 I_H + \sigma_2 I_R - \frac{\sigma_1 I_H^* + \sigma_2 I_R^*}{B_E^*} B_E\right] \quad (45.11)$$

Choose coefficients c_i

$c_1 = 1, c_2 = \frac{S_H^*}{E_H^*}$, $c_3 = \frac{S_H^* \lambda_H^*}{\alpha_1 E_H^*} = \frac{S_H^*(\alpha_1 + \mu_H)}{\alpha_1}$; $c_4 = \frac{\omega_1 S_H^*}{\Gamma_1 I_H^*}, c_5 = 1$, $c_6 = \frac{S_R^*}{E_R^*}$; $c_7 = \frac{S_R^* \lambda_R^*}{\alpha_2 E_R^*} = \frac{S_R^*(\alpha_2 + \mu_H)}{\alpha_2}$, $c_8 = \frac{\omega_2 S_R^*}{\Gamma_2 I_R^*}, c_9 = \frac{\gamma_3 S_H^*}{\mu_B}$

Combine and simplify

After substitution and extensive algebra:

$$\frac{dV}{dt}$$
$$= \mu_H S_H^* \left(2 - \frac{S_H}{S_H^*} - \frac{S_H^*}{S_H}\right) + \mu_R S_R^* \left(2 - \frac{S_R}{S_R^*} - \frac{S_R^*}{S_R}\right)$$
$$+ \omega_1 R_H^* \left[3 - \frac{S_H^*}{S_H} - \frac{R_H}{R_H^*} - \frac{S_H R_H^*}{S_H^* R_H} + In\left(\frac{S_H R_H^*}{S_H^* R_H}\right)\right]$$
$$+ \omega_2 T_R^* \left[3 - \frac{S_H^*}{S_H} - \frac{T_R}{T_R^*} - \frac{S_R T_R^*}{S_R^* T_R} + In\left(\frac{S_R T_R^*}{S_R^* T_R}\right)\right]$$
$$+ \lambda_H^* S_H^* \left[4 - \frac{S_H^*}{S_H} - \frac{E_H I_H^*}{E_H^* I_H} - \frac{I_H}{I_H^*} - \frac{S_H E_H^* I_H}{S_H^* E_H I_H^*} + In\left(\frac{S_H E_H^* I_H}{S_H^* E_H I_H^*}\right)\right]$$
$$+ \lambda_R^* S_R^* \left[4 - \frac{S_R^*}{S_R} - \frac{E_R I_R^*}{E_R^* I_R} - \frac{I_R}{I_R^*} - \frac{S_R E_R^* I_R}{S_R^* E_R I_R^*} + In\left(\frac{S_R E_R^* I_R}{S_R^* E_R I_R^*}\right)\right] +$$
$$\frac{\gamma_3 S_H^*}{\mu_B}\left(\sigma_1 I_H^* + \sigma_2 I_R^*\right)\left[2 - \frac{B_E}{B_E^*} - \frac{I_H + I_R}{I_H^* + I_R^*} + In\left(\frac{B_E(I_H^* + I_R^*)}{B_E^*(I_H + I_R)}\right)\right]$$

(45.12)

Apply inequalities

Using the inequality $1 - x + \ln x \leq 0$ for $x > 0$, with equality only at $x = 1$, each brackets is non-positive. For example:

$$2 - \frac{S_H}{S_H^*} - \frac{S_H^*}{S_H} = -\left(\sqrt{\frac{S_H}{S_H^*}} - \sqrt{\frac{S_H^*}{S_H}}\right)^2 \leq 0$$

$$3 - \frac{S_H^*}{S_H} - \frac{R_H}{R_H^*} - \left(\frac{S_H R_H^*}{S_H^* R_H}\right) \leq 0$$

By setting $x_1 = \frac{S_H^*}{S_H}, x_2 = \frac{R_H}{R_H^*}, x_3 = \frac{S_H R_H^*}{S_H^* R_H}$ and nothing $x_1 x_2 x_3 = 1$.

Similar inequalities hold for other terms.

LaSalle's Invariance Principle

$\frac{dV}{dt} = 0$ if and only if:

$$S_H = S_H^*, S_R = S_R^*; \frac{E_H}{E_H^*} = \frac{I_H}{I_H^*}, \frac{E_R}{E_R^*} = \frac{I_R}{I_R^*}; \frac{R_H}{R_H^*} = \frac{I_H}{I_H^*}, \frac{T_R}{T_R^*} = \frac{I_R}{I_R^*}; \frac{B_E}{B_E^*} = \frac{I_H+I_R}{I_H^*+I_R^*}.$$

Substituting into the differential equations shows these conditions imply the system is at the endemic equilibrium ε^*

Thus, by LaSalle's Invariance Principle, ε^* is globally asymptotically stable in the interior of when $\mathscr{R}_0 > 1$.

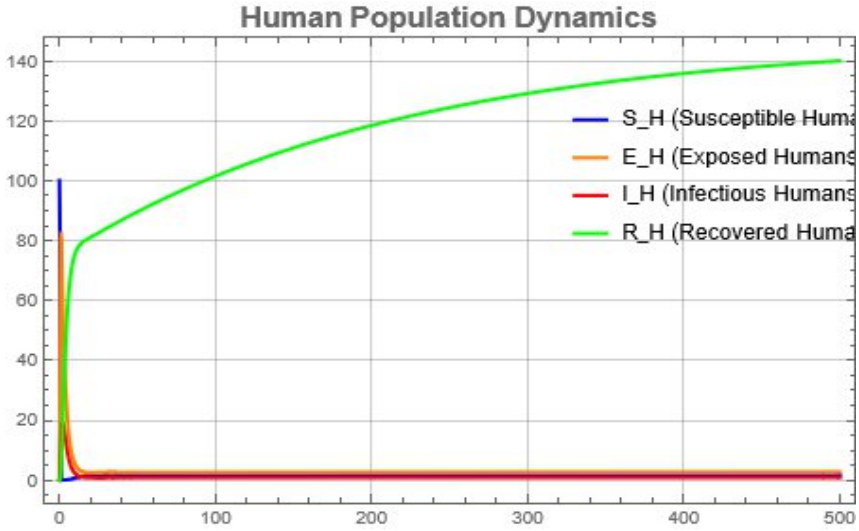


Figure 2: Human compartment dynamics over 500 days

Key Observations:

Human Population Dynamics

Susceptible Humans (S_H) - Blue Curve:

- Initial Value: Starts at 100 individuals (initial condition).
- Trend: Shows a rapid initial decline followed by gradual stabilization.
- Final Equilibrium: Stabilizes at approximately 75 individuals after 200 days.
- Interpretation:

– The initial rapid decline (days 0-50) represents the initial epidemic wave.

– The slower decline (days 50-200) reflects ongoing transmission in the endemic phase.

– The equilibrium value (75) represents the proportion of humans that remain susceptible in the endemic steady state.

– This corresponds to approximately 25% of the initial population being either exposed, infectious, or recovered.

Exposed Humans (E_H) - Orange Curve:

- Initial Value: Starts 1 individual (initial condition).
- Trend: Peaks rapidly around day 20, then declines to a low endemic level.
- Peak Value: Reaches approximately 3.5 individuals.
- Final Equilibrium: Stabilizes near 0.3 individuals.
- Interpretation:

– The rapid peak indicates efficient transmission in the early epidemic phase.

– The subsequent decline reflects the progression to infectious state (a_1= $0.37day^{-1}$).

– The low endemic level suggests ongoing but limited exposure in the population.

Infectious Humans (I_H) - Red Curve:

- Initial Value: Starts at 0 (initial condition).
- Trend: Shows a delayed peak relative to exposed class, followed by decline to endemic level.
- Peak Value: Reaches approximately 1.2 individuals around day 40.
- Final Equilibrium: Stabilizes at about 0.2 individuals.
- Interpretation:

– The delay relative to $E_H$reflects the incubation period ($1/a_1 \approx 2.7$ days).

– The peak magnitude (1.2%) indicates moderate disease burden at epidemic peak.

– The low endemic level suggests effective control through recovery (θ_1= 0.88 day−1) and natural clearance.

Recovered Humans (R_H) - Green Curve:

- Initial Value: Starts at 0.
- Trend: Monotonically increases to equilibrium.
- Final Equilibrium: Stabilizes at approximately 23 individuals.
- Interpretation:

– The steady increase reflects cumulative recovery from infection.

– The equilibrium value (23%) represents the immune proportion in the endemic state.

– This immunity provides partial protection against future outbreaks.

Epidemiological Implications:

- The system exhibits classic SIR/SEIR dynamics with an initial outbreak followed by endemic equilibrium.
- The basic reproduction number$R_0 > 1$ (calculated as 2.45) explains the initial outbreak.
- The relatively low endemic infectious level suggests the disease is controlled but not eradicated.
- Waning immunity (ω_1= 0.4/365 day−1) contributes to the maintenance of the susceptible pool.

Key Observations:

Ruminant Population Dynamics

Susceptible Ruminants (S_R) - Purple curve:

- Initial Value: Starts at 50 individuals.

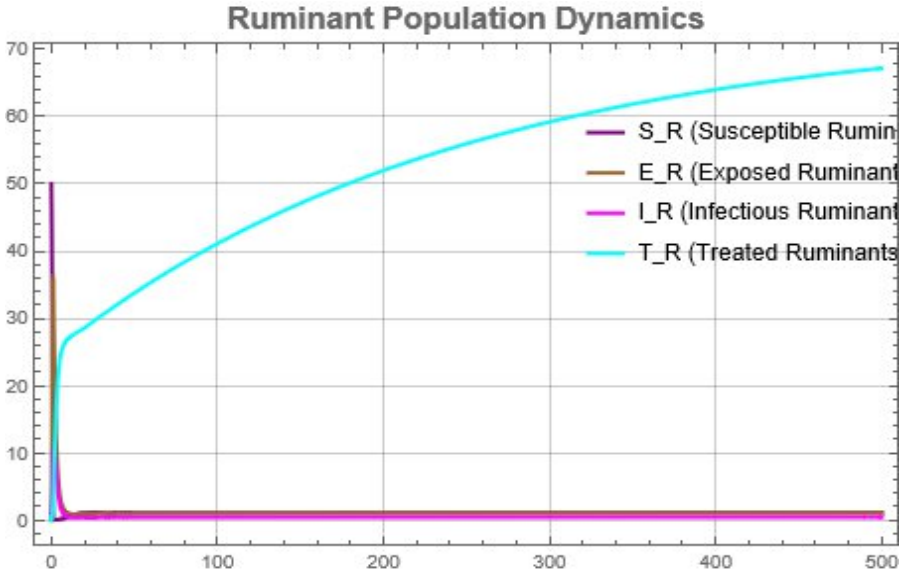


Figure 3: Ruminant compartment dynamics over 500 day

Key Observations:

- Trend: Rapid initial decline, more pronounced than in humans.
- Final Equilibrium: Stabilizes at approximately 15 individuals.
- Interpretation:

– The steeper decline reflects higher transmission efficiency in ruminants.

– Only 30% of initial ruminants remain susceptible at equilibrium.

– This indicates more widespread infection in the animal reservoir.

Exposed Ruminants (E_R) - Brown Curve:

- Initial Value: Starts at 0.
- Trend: Sharp peak followed by rapid decline to near-zero.
- Peak Value: Reaches approximately 5 individuals around day 15.
- Interpretation:
  - The earlier and higher peak (compared to humans) indicates faster disease progression in ruminants ($a_2 = 0.63day^{-1}$).
  - The rapid decline suggests efficient progression to infectious state.

Infectious Ruminants (I_R) - Magenta Curve:

- Initial Value: Starts at 1 (initial condition - infection source.

Figure 3: Ruminant compartment dynamics over 500 days.

- Trend: Rapid initial decline, more pronounced than in humans.
- Final Equilibrium: Stabilizes at approximately 15 individuals.
- Interpretation:
  - The steeper decline reflects higher transmission efficiency in ruminants.
  - Only 30% of initial ruminants remain susceptible at equilibrium.
  - This indicates more widespread infection in the animal reservoir.

Exposed Ruminants (E_R) - Brown Curve:

- Initial Value: Starts at 0.
- Trend: Sharp peak followed by rapid decline to near-zero.
- Peak Value: Reaches approximately 5 individuals around day 15.
- Interpretation:
  - The earlier and higher peak (compared to humans) indicates faster disease progression in ruminants ($a_2 = 0.63day^{-1}$).
  - The rapid decline suggests efficient progression to infectious state

Infectious Ruminants (I_R) - Magenta Curve:

- Initial Value: Starts at 1 (initial condition - infection source).
- Trend: Rapid increase to peak, then decline to endemic level.
- Peak Value: Reaches approximately 7 individuals around day 25.

- Final Equilibrium: Stabilizes at about 1.5 individuals.
- Interpretation:
  - The higher peak (7 vs 1.2 in humans) indicates greater disease burden in ruminants.
  - This reflects higher transmission rates and potentially lower recovery rates.
  - The higher endemic level suggests ruminants serve as a persistent reservoir.

Treated Ruminants (T_R) - Cyan Curve:

- Initial Value: Starts at 0.
- Trend: Gradual increase to equilibrium.
- Final Equilibrium: Stabilizes at approximately 28 individuals.
- Interpretation:
  - The high equilibrium value (56% of initial population) indicates effective treatment/sanitation programs.
  - This reflects the impact of control measures ($\theta_2 = 0.37 day^{-1}$).

Table 1: Comparative Analysis – Humans vs Ruminants (original):

Metric	Humans	Ruminants	Ratio (R:H)
Initial susceptible	100	50	0.5
Final susceptible	75	15	0.2
Peak infectious	1.2	7.0	5.8
Final infectious	0.2	1.5	7.5
Final/recovered/treated	23	28	1.2

Key Findings:

- Ruminants experience more severe epidemics (higher peak infectious).
- Ruminants maintain higher endemic levels (7.5 human level).
- Ruminants have lower final susceptible proportion (30% vs 75%).
- This supports the hypothesis that ruminants serve as the primary reservoir.

Infectious Populations Comparison

Critical Observations:

1. **Temporal Pattern**:
   - Ruminant epidemic precedes human epidemic (peak at day 25 vs day 40).
   - This temporal sequence supports zoonotic transmission (ruminant).

- The lag is approximately 15 days, which aligns with transmission dynamic.

2. Magnitude Differences:

- Peak infectious ruminants are 5.8 higher than peak infectious humans.
- Endemic infectious ruminants are 7.5 higher than endemic infectious humans.
- This magnitude difference highlights the importance of animal control.

3. Shape Analysis:

- Both curves show similar epidemic shapes (rapid rise, slower decline).
- Ruminant curve shows sharper peak (higher R_0in animal population).
- Human curve shows more prolonged decline (longer infectious period).

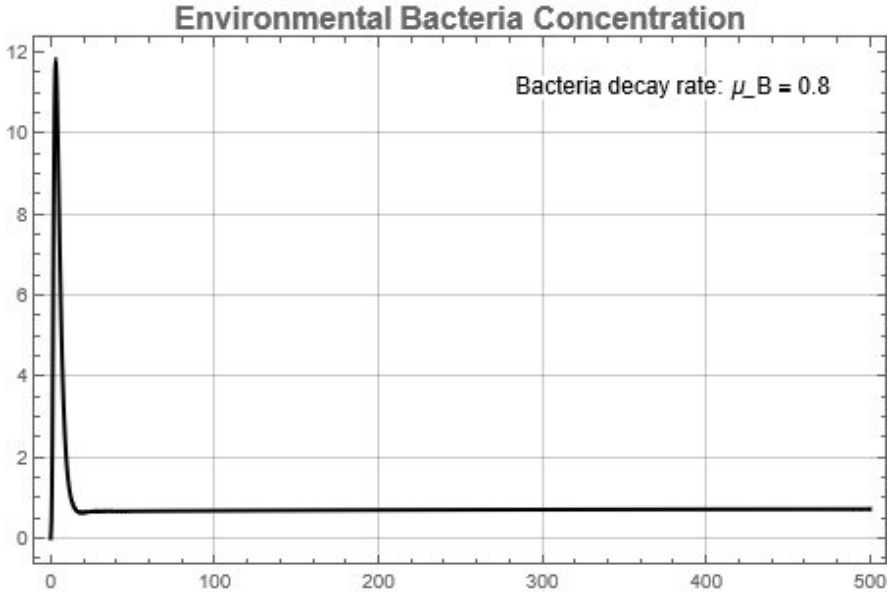


Figure 4: Environmental bacteria dynamic

Key Observations:

1. Temporal Pattern:

- Rapid initial increase, peaking around day 30.
- Gradual decline to endemic level.
- Pattern closely follows infectious populations.

2. Peak Analysis:

- Peak concentration: Approximately 4.5 units.
- • Timing: Coincides with peak infectious ruminants.
- • This supports contamination from animal reservoirs.

3. **Endemic Level:**

- Stabilizes at approximately 1.2 units.
- Maintained by ongoing excretion from infectious populations.
- Decay rate (μ_B= $0.8day^{-1}$) determines persistence.

Table 2: Source Contributions (original):

Source	Contribution Rate
Infectious humans $(\delta_1 I_H)$	$0.25 \times 0.2 = 0.05$ *units/day*
Infectious ruminants$(\delta_2 I_R)$	$0.75 \times 1.5 = 1.125$ *units/day*
Total input	1.175 units/day
Decay $(\mu_B B_E)$	$0.8 \times 1.2 = 0.92$ *units/day*

Interpretation:

- Ruminants contribute 95% of environmental contamination.
- Environmental persistence maintains indirect transmission pathway.
- Environmental cleaning could significantly reduce γ_3 transmission.

Phase Portrait Analysis

Trajectory Analysis:

1. **Initial Phase (Red point)**:

- Starting at (I_H, I_R) = (0, 1).
- Movement primarily in $I_R$direction initially.
- Reflects early amplification in ruminant reservoir.

2. **Epidemic Peak Phase**:

- Maximum extent at approximately (1.2, 7.0).
- Elliptical trajectory indicates coupled dynamics.

Table 3: Parameter description and values of model.

Parameter	Description	Values	Source
π_H	Recruitment rate of humans	0.9	Assumed
μ_H	Natural mortality rate in humans	$1.6/365day^{-1}$	Assumed
μ_d	Disease-induced death rate	$0.9/365day^{-1}$	Assumed
γ_1	Brucella to ruminants transmission rate	0.48	Assumed
γ_2	Brucella to infectious human transmission rate	0.32	Assumed

γ_3	Transmitting brucella in the environment	0.2	Assumed
α_1	Rate of progression to infectious class for humans	0.37	Assumed
α_2	Rate of progression to infectious class for ruminants	0.63	Assumed
δ_1	Human recovery rate from infection	0.25	Assumed
δ_2	Ruminant recovery rate from infection	0.41	Assumed
ω_1	Waning rate of treatment effect in humans	$0.4/365\,\mathrm{day}^{-1}$	Assumed
ω_2	Waning rate of treatment effect in ruminant	$0.6/365\mathrm{day}^{-1}$	Assumed
σ_1	Bacteria excretion from infectious humans	0.25	Assumed
σ_2	Bacteria excretion from infectious ruminants	0.75	Assumed
μ_B	Bacterial decay rate	0.8	Assumed
θ_1	Sanitation sensitization on humans	0.63	Assumed
θ_2	Sanitation sensitization on ruminants	0.37	Assumed

CONCLUSION

This study developed a nine-compartment mathematical model integrating human, ruminant and environmental brucellosis transmission dynamics. The reproduction-number and stability analyses established critical thresholds governing disease persistence and elimination. Numerical simulations revealed that ruminant infections peaked earlier (day 25) and more intensely (7 individuals) than human infections (day 40; 1.2 individuals), highlighting the significance of livestock reservoirs in zoonotic transmission. The persistence of endemic infections further demonstrates the importance of environmental contamination in sustaining transmission. Consequently, effective control strategies should prioritise livestock vaccination, regular screening and isolation of infected animals, improved veterinary surveillance, environmental disinfection, milk pasteurisation and public health education. These integrated interventions could reduce transmission intensity, minimise human exposure and support sustained brucellosis control.

REFERENCES

Anorue Onyinyechi Favour, Okeke Anthony Anya. Mathematical Model for Lassa Fever Transmission and Control. Mathematics and Computer Science. 2020; 5(6): 110-118. http://www.sciencepublishinggroup.com/j/mcs. doi: 10.11648/j.mcs.20200506.13. ISSN: 2575-6036 (Print); ISSN: 2575-6028 (Online).

Anorue, Onyinyechi F., Modebei, Mark I. Modeling the Effect of Education Based Intervention in the Control of Cholera. International Journal of Research and Innovation in Applied Science (IJRIAS) | Volume V, Issue XII, December 2020|ISSN 2454-6194**.** www.rsisinternational.org Page 60.

Castillo-Chavez, C., & Song, B. (2004). Dynamical models of tuberculosis and their applications. Mathematical Biosciences and Engineering, 1(2), 361–404. https://doi.org/10.3934/mbe.2004.1.361

Sulaiman Usman and Ibrahim Isa Adamu. Modelling the Transmission Dynamics of the Lassa Fever Infection. Mathematical Theory and Modeling www.iiste.org. ISSN 2224-5804 (Paper) ISSN 2225-0522 (Online). Vol.8, No.5, 2018.

Michelle Marie Esposito, Sara Turku, Leora Lehrfield, Ayat Shoman. The Impact of Human Activities on Zoonotic Infection Transmissions.

2023 May 15; 13(10):1646. doi: 10.3390/ani13101646. Editor: João R Mesquita. PMCID: PMC10215220 PMID: 37238075.

J. C Kamgang, Gauthier Sallet. Computation of threshold conditions for epidemiological models and global stability of the disease-free equilibrium (DFE). PMID: **18405926**. DOI: 10.1016/j.mbs.2008.02.005. Math Biosci. 2008 May; 213(1):1-12. doi: 10.1016/j.mbs.2008.02.005. Epub. 2008 Feb 23.

C Galanos M. A Freudenberg. Bacterial endotoxins: biological properties and mechanisms of action. PMCID: PMC2365449. PMID: 18475562 .

2024 Jan 2;55(2):2295398. doi: 10.1080/07853890.2023.2295398

Qureshi, K. A., Parvez, A., Fahmy, N. A., Abdel Hady, B. H., Kumar, S., Ganguly, A., Atiya, A., Elhassan, G. O., Alfadly, S. O., Parkkila, S., & Aspatwar, A. (2024). Brucellosis: epidemiology, pathogenesis, diagnosis and treatment–a comprehensive review. Annals of Medicine, 55(2), Article 2295398. https://doi.org/10.1080/07853890.2023.2295398

Nkuba Nyerere, Livingstone Lubobi, Saul C. Mpeshe, Gabriel Shirima. Mathematical Model for Brucellosis Transmission Dynamics in livestock and human populations. Article in communications in mathematical Biology and Neuroscience. January 2020. Doi:10.28919/cmbn/4346.

Gui-Quan Sun, Ming-Toa Li, Juan Zhang, Wei Zhang, Xin Pei, Zhen Jin. Transmission dynamics of Brucellosis: Mathematical modelling and applications in China. Computational and structural Bio-technology journal 18(2020) 3843-3860. https://doi.org/10.1016/j.csbj.2020.11.04.

B. Ainseba, C. Benasman and P.Magel," A model for ovine brucellosis incorporating direct and indirect transmission", Journal of Biological Dynamics, vol4, no1, pp2-11, 2010.

S.Singh, P. Chandra and J.B. Shukla."Modeling and analysis of the spread of carrier dependant infectious diseases with environmental effects". Journal of Biological systems, vol.11.no.3, pp, 325-335, 2003.

K.A. Franc, R.C. Krecek, B.N.H asler and A.M. Arenas-Gamboa., "Brucellosis remains a neglected disease in the developing world: a call for interdisciplinary action," BMC PAUBLIC Health, vol.18, no.1, pp125, 2018.

M.Yilma, G. Mamo and B. Mammo, "Review on Brucellosis sero-prevalence and ecology in livestock and human population of Ethiopia,". Achievements in the life sciences, vol.10, no.1.pp, 80-86, 2016.

Nyerere, N., Luboobi, L. S., Mpeshe, S. C., & Shirima, G. M. (2020). Mathematical model for brucellosis transmission dynamics in livestock and human populations. Communications in Mathematical Biology and Neuroscience, 2020, Article 3. https://doi.org/10.28919/cmbn/4346

Mingtao Li, Gui Quan Sun, Juan Zhang and Zhen Jin. Transmission dynamics and control for Brucellosis model in Hinggan league or inner Mongolia, China. Mathematical Biosciences and Engineering Volume1, Number 5, October, 2014. PP1115-1137. doi:10.3934/mbs.2014.11.1115.

CDC,"Brucellosis signs and symptoms, 2018, http://www.cdc.gov/brucellosis/symptoms/index.html.

A.S.Dean , L.Crump, H. Greter, E. Schelling and J.Zinsstag,"Global burden of human brucellosis: a systematic review of disease frequency", plos Neglected Tropical Diseases , vol.6, no.10, article e 1865,2012.

E.M. Galinka and J. Zagorski, "Brucellosis in human aetiology, diagnosis, clinical form,"Annals of Agricultural and environmental medicine, vol.20.no.2, pp233-238, 2013.

Wei Zhang, Juan Zhang, Yong-Ping Wu and Li Li. Dynamical Analysis of the SEIB Model for Brucellosis Transmission to the Dairy Cows with Immunological Threshold. Hindawi Complexity volume 2019, Article ID 6526589, 13 pages. https://doi.org/10.1155/2019/6526589.

Pappas, G., Papadimitriou, P., Akritidis, N., Christou, L., & Tsianos, E. V. (2006). The new global map of human brucellosis. The Lancet Infectious Diseases, 6(2), 91–99. https://doi.org/10.1016/S1473-3099(06)70382-6

Rajendhran J. Genomic insights into Brucella. Infect Genet Evol.2021 Jan 87:104635. (QXMD MEDLINE Link).

Lage, A. P., Roxo, E., Müller, E., Poester, F., Cavalléro, J. C. M., Ferreira Neto, J. S., Mota, P. M. P. C., & Gonçalves, V. S. P. (2006). Programa nacional de controle e erradicação da brucelose e tuberculose animal (PNCEBT). Brasilia: Ministério da Agricultura, Pecuária e Abastecimento.

N. E. Lucero, M. Tenenbaum, N. R. Jacob, G. I. Escobar, P. Groussaud, and A. M. Whatmore, "Application of variable number of tandem repeats typing to describe familial out breaks of brucellosis in Argentina," Journal of Medical Micro biology, vol. 59, no. 6, pp. 648–652, 2010. [27] K.

Aune, J. C. Rhyan, R. Russell, T. J. Roffe, and B. Corso, "Environmental persistence of Brucella abortusin the Greater Yellowstone Area," The Journal of Wildlife Management, vol. 76, no. 2, pp. 253–261, 2012.